Available online at www.sciencedirect.com
ScienceDirect
Acta Biomaterialia xxx (2007) xxx–xxx
Acta BIOMATERIALIA
www.elsevier.com/locate/actabiomat

Assessment of tissue scaffold degradation using electrochemical techniques

Alison Willows [a,*], Qiang Fan [b], Fanya Ismail [b], Claudia M. Vaz [c], Paul E. Tomlins [c], Lyuba I. Mikhalovska [a], Sergey V. Mikhalovsky [a], Stuart L. James [a], Pankaj Vadgama [b]

[a] School of Pharmacy and Biomolecular Sciences, University of Brighton, Lewes Road, Brighton BN2 4GJ, UK
[b] IRC in Biomedical Materials, Queen Mary University of London, Mile End Road, London E1 4NS, UK
[c] Division of Engineering and Process Control, National Physical Laboratory, Hampton Road, Teddington TW11 0LW, UK

Received 9 March 2007; received in revised form 12 October 2007; accepted 19 October 2007

Abstract

Degradation of a commercially available collagen–glycosaminoglycan dermal equivalent matrix was studied using electrochemical techniques. Degradation was accelerated by exposure to gamma radiation followed by storage at elevated temperatures or exposure to enzymes. The time-dependent diffusion of a small, electrochemically active, molecular probe, potassium ferrocyanide, through the matrix was monitored via changes in the oxidation peak currents of cyclic voltammograms. These measurements were made using a two-compartment diffusion chamber with the sample positioned well away from the working electrodes and a single-compartment electrode cell where the matrix was in direct contact with the working electrode. The relative merits of these two approaches are considered. Regardless of the approach chosen, amperometry appears well suited to monitoring progressive diffusivity changes through mechanically weak porous structures subject to different solution environments.

Keywords: Tissue scaffold; Degradation; Electrochemistry; Porous structure; Amperometry

1. Introduction

Tissue scaffolds are designed to provide temporary, degradable matrices for supporting cells to grow new, functional living tissue. The materials from which such scaffolds are manufactured range from hard inorganic materials, such as hydroxyapatite, to highly hydrated gel-like materials, depending on the intended application. Scaffold materials can be either synthetic or biologically derived. Whilst synthetic materials can be manufactured with predictable and reproducible chemical, mechanical and physical characteristics, they may elicit unexpected biological responses when in contact with tissues. Hence, there is continuing interest in bioderived materials such as collagen which, as natural interstitial tissue components, provide a viable alternative route to producing biocompatible tissue scaffolds [1,2]. To date there is no consensus as to which are the "best" materials to use for a particular application, which structures provide the optimal environment for cell growth or what are the most appropriate mechanical and chemical properties for the cell microenvironment.

Understanding the basic structure of complex tissue scaffolds has proved to be challenging, especially for highly hydrated soft materials such as gels, together with the quantitative determination of how these structures degrade with time. The latter is key to the development for optimizing scaffold designs based on biodegradable materials. Indeed, many of the commonly used structural evaluation tools, such as X-ray micro-computer tomography [3–5], mercury porosimetry [4] and capillary flow porometry, cannot be used on gel-like materials due to their softness or lack of contrast. Some useful information can be obtained through the analysis of electron micrographs [5], but this

* Corresponding author. Tel.: +44 1273 642036; fax: +44 1273 679333.
E-mail address: a.d.willows@brighton.ac.uk (A. Willows).

1742-7061/$ - see front matter © 2007 Published by Elsevier Ltd. on behalf of Acta Materialia Inc.
doi:10.1016/j.actbio.2007.10.009

has a strong dependence on the preparative method. A feasible procedure used to investigate the structure of gels is neutron scattering, which enables analysis under near-physiological conditions and thus allows a hydrated gel to be examined [6,7]. However, this cannot be classed as a routine method due to the availability of equipment required for the analysis.

A more pragmatic approach to characterizing gels is to measure the diffusivity of molecular probes through the material as a function of different environmental conditions and time. This approach has been recently explored using cyclic voltammetry and shown to be a viable non-invasive method [8].

In this paper we have extended this study to investigate different sample cells for monitoring probe diffusion through scaffold materials and to explore the effect that accelerated degradation has on in vitro permeability. The material used is a commercially available collagen-based material used as a dermal substitute. Collagen-based matrices are materials commonly used for skin, connective tissue and peripheral nerve tissue engineering applications [1,2]. These materials have an obvious physiological advantage over synthetic polymers, given their derivation from natural tissue. The relationship between the initial structure and the degradation performance over time is key to the success of the scaffold. Understanding the kinetics of degradation in a cell-seeded scaffold is by no means intuitive as there are many key factors that need to be considered in a passive, i.e. non-mechanically stimulated, system, including the presence of extracellular matrix, changes in the structure of the material, the cell density and perfusion characteristics, and the concentration of relevant enzymes. This was understood in the development of collagen-based tissue engineering scaffolds [9]. More recently, Jarman-Smith et al. [10] have demonstrated that heavily cross-linked porcine dermal collagen was very resistant to collagenases, but was also impenetrable to dermal fibroblasts, and thus cellular infiltration of such scaffolds will not occur. Harley et al. [11], using collagen guide chambers as conduits for nerve regeneration, showed that increasing the cross-link density within the collagen decreased the degradation rate and that nerve regeneration quality reached an optimum at a degradation rate which gave a chamber half-life of 2–3 weeks in vivo. Similarly, Gordon et al. [12] suggested that chondrocytes growing in fast degrading collagen scaffolds grew less well than in those degrading less quickly. These authors did, however, suggest that some uncoupling of scaffold degradation and tissue regeneration may occur.

Degradation of collagen-based scaffolds in vivo is likely to be due to a number of physiochemical and biological effects. In particular, the matrix metalloproteinase MMP-8 (neutrophil collagenase) is likely to play a dominant role. Van Amerongen et al. [13] have shown that a collagen scaffold used in the experimental reconstruction of murine myocardium becomes surrounded by neutrophils at about day 14 in vivo, and that MMP-8 co-localizes with the neutrophils, suggesting that much of the collagen degradation is enzymic. Exposure to ultraviolet or gamma radiation is a commonly used method in medicine for sterilizing materials. Indeed, this is often the only route for sterilizing materials that are thermally sensitive and contain significant amounts of water. This approach has a drawback in that radiation exposure can lead to chain scission or cross-linking of polymers [14,15]. The former effect has been well-documented for medically relevant materials such as poly(-methyl methacrylate) and polyethylene, but less well so for natural materials such as collagen [16,17]. Radiation can induce structural changes in materials that may impact on their performance, i.e. mechanical properties enhanced through cross-linking or reduced by chain scission.

Various approaches have been used to accelerate degradation of naturally occurring polymers; Pek et al. [18] reported the use of enzymes such as collagenase and chondroitinase to degrade a collagen–glycosaminoglycan (C-GAG) skin substitute. Holy et al. [19] used pH change as a means of accelerating the rate of degradation in PLGA (poly(lactic-*co*-glycolic acid) scaffolds. Their results show that the rate of degradation of PLGA increased at lower pH, although this was not quantified.

Determination of scaffold degradation is most commonly accomplished using histological, immunocytochemical or other ultrastructural methods [18,20], but this is poorly quantifiable, prompting the current study. In this paper we have used cyclic voltammetry to study changes in the diffusion behaviour of ferri/ferrocyanide through collagen-based scaffolds that have been subjected to different doses of gamma radiation followed by accelerated ageing at elevated temperatures or in the presence of enzymes (collagenase) or at different pHs.

2. Materials and methods

2.1. Model membranes

Nuclepore® polycarbonate membranes (Whatman, UK) with pore sizes 0.05, 5 and 12 μm were used as control matrixes as they have sharply defined pore sizes and good chemical resistance.

2.2. Tissue scaffold

A commercially available collagen cross-linked with glycosaminoglycan (C-GAG) dermal equivalent scaffold (Integra® Bilayer Matrix Wound Dressing), of nominal thickness 1.5 mm, was removed from storage in 70 vol.% isopropanol (IPA) and cut into approximately 10 mm × 10 mm squares prior to being irradiated. A protective backing silicone layer that was attached to one side of the hydrogel matrix was carefully removed prior to use in experiments and before any radiation exposure. The manufacturers state that the C-GAG scaffold has a pore volume fraction of 98%, with average pore diameter

Please cite this article in press as: Willows A et al., Assessment of tissue scaffold degradation using ..., Acta Biomater (2007), doi:10.1016/j.actbio.2007.10.009

in the range 30–120 μm. The in vivo degradation rate is 30 days and the storage shelf-life is 24 months.

2.3. Exposure to gamma radiation

Two groups of C-GAG samples were sealed in small glass containers in the presence of 70/30 IPA/water mixture and irradiated at room temperature using a source with an average homogeneous dose power of 1 kGy h^{-1}. The exposure levels for each sample were 25 and 50 kGy, respectively. An exposure level of 25 kGy is considered to be the reference absorbed dose for medical sterilization [21]. An exposure level of 50 kGy was also used to investigate the effect of higher levels of irradiation than the minimum. Non-irradiated samples were used as controls.

2.4. Degradation studies

Gamma-irradiated C-GAG samples (γ-C-GAG) were removed from the IPA/water solution and thoroughly rinsed for 1 min in phosphate-buffered saline (PBS) prior to application. All chemicals used were analytical grade or equivalent and used as received.

2.4.1. Temperature effect

γ-C-GAG samples were immersed in PBS at physiological pH (pH 7.4) and incubated for periods of 12, 24 and 48 h at two different temperatures: (i) $T = 37$ °C and (ii) $T = 44$ °C (to simulate possible inflammatory conditions).

2.4.2. Enzymatic degradation

γ-C-GAG samples were immersed in PBS containing two different collagenase (Sigma–Aldrich, UK) concentrations: (i) 5 μg ml^{-1} and (ii) 10 μg ml^{-1}. The samples were incubated for periods of 12, 24 and 48 h under physiological conditions (37 °C and pH 7.4). After the incubation period, the samples were removed from the solutions, rinsed thoroughly with deionized water and stored in a 70/30 IPA/water mixture until required.

2.4.3. pH effect

γ-C-GAG samples were immersed in phosphate-buffered solution (made using PBS tablets, Aldrich) and stored at 37 °C at two different pHs: pH 7.4 (physiological conditions) and pH 5 (potential inflammatory conditions). Samples were incubated for 12, 24 and 48 h, respectively.

2.5. Scanning electron microscopy

Scanning electron microscopy (SEM) of the reference G-GAG and hydrogels treated by gamma radiation and by collagenase were performed. Specimens of G-GAG were dehydrated by a series of acetone dilutions followed by critical point drying. Finally, specimens were gold sputtered and analysed using a 6310 JEOL microscope.

2.6. Cyclic voltammetry

In a recent study [8] we developed the use of a small molecule redox couple, ferri/ferrocyanide, as a probe for diffusion characterization. Ferri/ferrocyanide is a classical, reversible molecular probe used in conventional electrochemistry as a basis for characterizing diffusion reactions at electrode surfaces. Such measurements can be used to determine the effective diffusion coefficient for the molecular probe through a porous material. There are many other well-documented redox systems that can be considered as a standard, but the ferri/ferrocyanide used in this investigation [22] is readily monitored using a standard platinum electrode;

$$\mathrm{Fe(CN)_6^{4-}} \Longleftrightarrow \mathrm{Fe(CN)_6^{3-}} + \mathrm{e^-}, \quad E^0 = +0.36\ \mathrm{V\ vs\ NHE} \tag{1}$$

Here the NHE is the normal hydrogen electrode against which all standard potentials (E^0) are related. Under conventional solution conditions, this redox couple has fast electron transfer kinetics and is a simple single electron reaction without any additional side reactions, giving rise to well-defined single oxidation and reduction peaks during cyclic voltammetry [23]. This particular redox couple is especially useful for investigating different electrode surfaces as the solution response is already well characterized. Potassium ferrocyanide (MW = 422.41), although not physiologically relevant, can be used as a molecular probe to assess the porous membrane permeability to microsolutes, as discussed below.

Two experimental approaches, shown in Figs. 1 and 2, were used to obtain cyclic voltammograms (CVs). In Fig. 1 the sample, after rinsing in distilled water and soaking in PBS buffer, was placed over a platinum (Pt) working electrode with a Pt wire as counter-electrode and an Ag/AgCl reference both immersed in the bulk solution above the membrane. The single-compartment electrochemical cell utilized a commercial measuring chamber, the Rank cell (Rank Brothers, Cambridge, UK). The sample was in contact with a 12 mm^2 working electrode. Samples were immersed in buffer and excess buffer was removed before adding an aqueous solution of 0.1 M potassium ferrocyanide ($K_4Fe(CN)_6$) in PBS at pH 7.4. A software controlled μAutolab II (Ecochemie, the Netherlands) potentiostat was used to record all voltammetric experiments with potentials recorded with respect to an Ag/AgCl electrode. Sequential recordings of the CVs were made taking the time at which the sample was exposed to the redox couple as time zero.

Alternatively, a sample with a diameter of 10 mm was used in a two-compartment diffusion cell shown in Fig. 2. Here, the sample was sandwiched between two sheets of a coarse mesh used for containing gel-like materials in size exclusion chromatography columns. The mesh served to support the sample and helped maintain a uniform thickness. The Pt working electrode was sited in chamber B, which initially contained only PBS buffer. The Pt wire

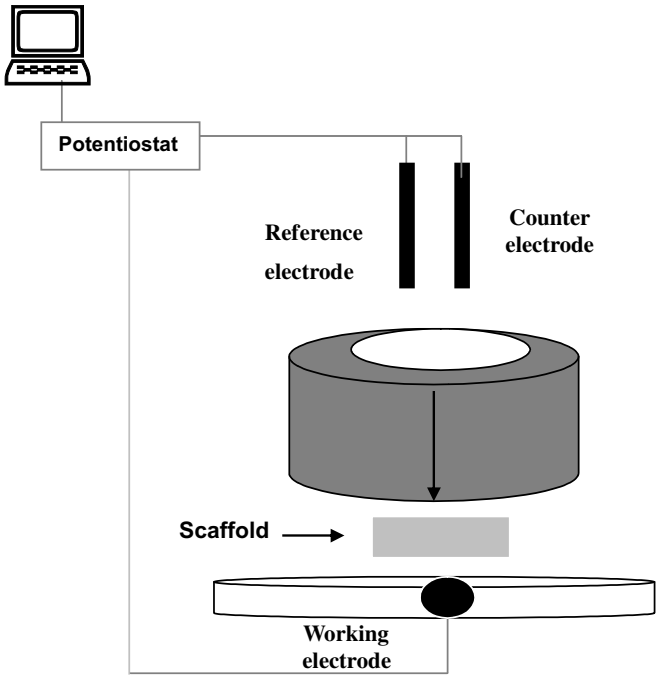

Fig. 1. Representation of the single-compartment cell (Rank Brothers) containing a sheet of C-GAG matrix in direct contact with the Pt working electrode.

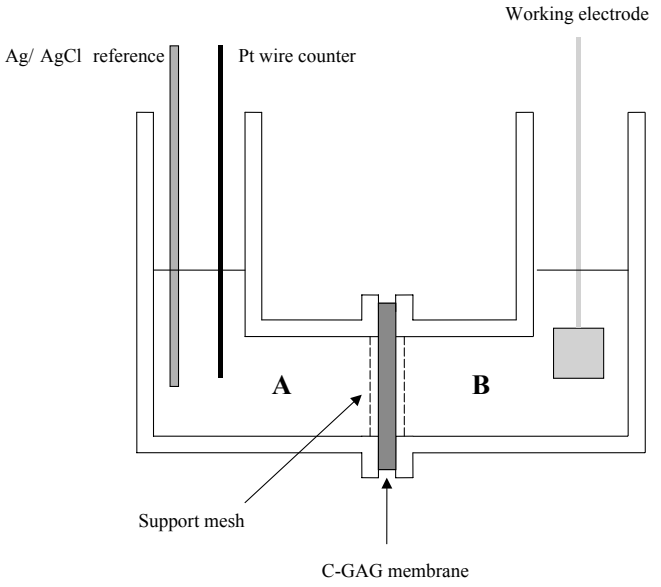

Fig. 2. Representation of the diffusion cell where a sheet of C-GAG matrix is sandwiched between two sheets of a coarse mesh. Initially chamber A contains the redox couple in PBS and chamber B contains only buffer.

counter-electrode and an Ag/AgCl reference electrode were placed in chamber A, which contained the redox couple dissolved in PBS. Care was taken to ensure that chambers A and B were filled with buffer and the buffer–redox couple, respectively, at the same rate and up to the same level. Care was also taken to ensure that the diffusion cell itself was level to avoid any undesirable bulk movement of fluid through the sample. Small magnetic stirrers were placed in each of the chambers to stop concentration gradients developing between measurements.

3. Results

3.1. Sensitivity of cyclic voltammograms to the electrolyte solution

In conventional electrochemical experiments the redox couple is dissolved in electrolyte solution, typically potassium chloride. The presence of the electrolyte ensures that solute ion mass transport due to migration is minimized and the effects of the electrode electric field are confined to a small distance from the surface. The supporting electrolyte needs to be inert in the potential range of the experiment and to carry the current of the electrochemical cell, thus minimizing any problems due to solution resistance. The electrolyte concentration in the PBS buffer (0.2 M) is lower than for the KCl experiments (1 M) and therefore there may be a contribution to the voltammogram from an effect due to a difference in the solution resistance.

Fig. 3 shows CVs obtained using the Rank cell shown in Fig. 1 in the presence of ferrocyanide in PBS and KCl, respectively. The results are typical of a single electron transfer process. The locations of the oxidation and reduction peaks are the same (+0.33 V for oxidation peak and +0.18 V for the reduction peak) between the two solutions, although there is a small increase in solution resistance when using PBS, shown by the increased background current. However, the voltammogram has good shape and current amplitude and, since the PBS system is closer to the buffer systems used elsewhere in this work, it was used for all electrochemical experiments.

3.2. Scan rate dependence of CVs in the Rank cell

Fig. 4 shows the sensitivity of the CVs to different scan rates for a control (a) and a non-irradiated C-GAG

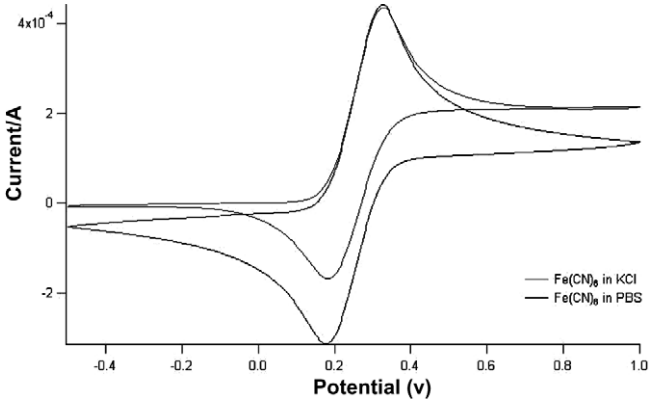

Fig. 3. Comparison of CVs measured in KCl and PBS in the absence of a sample measured using a scan rate of 100 mV s^{-1}.

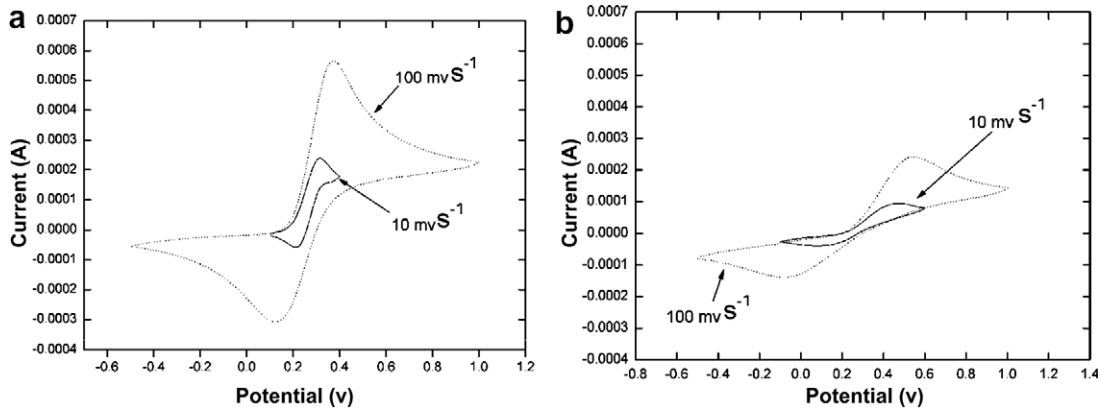

Fig. 4. The dependence of CVs on scan rate for (a) bare electrode and (b) C-GAG covered electrode using the single-compartment cell.

covered electrode (b). For a reversible reaction, such as that for the redox couple used here, the peak potential should be independent of the scan rate. The peak current should also be proportional to the square root of the scan rate. Both sets of voltammograms show that the oxidation and reduction peak positions change with the scan rate, so the system has deviated from its reversible characteristic at this electrode surface. Given that an essentially aqueous gel phase is in contact with the electrode, further alteration to the redox chemistry due to the gel is highly unlikely. This implies that the differences between the CVs for control and gel covered electrodes are due to changes in the diffusivity of the electroactive species. Whilst both the oxidation and reduction peak heights increase with increasing scan rate, if peak height is proportional to the square root of the scan rate, then a threefold increase in peak height would be expected for a scan rate change from 10 to 100 mV s^{-1}. There is, in fact, a loss of this relationship, confirming the loss of ideal reversible behaviour. However, the peak height for the control is also approximately twice that of the C-GAG-covered electrode. This is a clear indication that the sample retards the diffusion of ferrocyanide to the electrode surface. In order to avoid inconsistencies due to the electrode reaction, all subsequent measurements were made using a standard scan rate of 100 mV s^{-1}.

3.3. Comparison of experimental methods for determining CVs

The amplitude of the oxidation peak, i_p (A), in a cyclic voltammogram is proportion to the bulk concentration of the redox couple, C (mol cm^{-3}), according to the Randles–Sevčik equation [24]

$$i_p = (2.686 \times 10^5) n^{3/2} v^{1/2} D^{1/2} A C \quad \text{at } 25\,^{\circ}\text{C} \qquad (2)$$

where n is the number of electrons involved in the half reaction, D is the diffusion coefficient for solute migration to the electrode surface ($cm^2\ s^{-1}$), v is the scan rate (V s^{-1}) and A is the area of the electrode (cm^2). The constant, 2.686×10^5, applies at 25 °C. Eq. (2) can be applied to reversible electrode reactions and used to obtain estimates of D. The oxidation–reduction processes at the electrode surface for a simple redox reaction resulting from changes in the potential between the working and counter-electrode are diffusion limited. In practical terms, these reactions and ion movements during repeat scans take place within a boundary layer that extends some 200 nm away from the surface of the working electrode. For most of the experimental arrangements described here we can therefore assume that the diffusion coefficient for the redox couple will be the same as that for an aqueous solution, i.e. 7.6×10^{-6} $cm^2\ s^{-1}$ [23].

Fig. 5 shows the time-dependent evolution of CVs obtained from both the Rank cell (a) and the diffusion cell (b) during the first few minutes of exposing the C-GAG membrane to the redox couple. The amplitude of the current is much less in the diffusion cell system than in the Rank cell system, in fact by an order of magnitude. As the working electrodes used were matched for area, this difference must be due to the dilution of the redox couple by the buffer in chamber B. A practical consequence of these very weak currents is that data obtained at times below approximately 250 s were prone to excessive noise. The dilution problem could be overcome by doubling the concentration of ferrocyanide in the diffusion cell, but this would complicate comparisons of the two approaches through ionic strength effects in both the gels and the electrochemical reaction. Using a diffusion cell that contains smaller volumes of solution would also not readily solve the problem since proper sample immersion would be difficult. For this reason, the Rank cell method is more suitable for measuring solute diffusion through the C-GAG membrane, allowing lower probe solute concentrations to be utilized.

The time-dependent increase in the amplitude of the oxidation peak provides a direct route to monitoring the change in concentration of the redox couple in the immediate vicinity of the working electrode in line with Eq. (2). Fig. 6 shows a comparison of measurements obtained from the Rank cell system and the diffusion cell. From this figure it is clear that there is a marked difference in the results obtained using the Rank and diffusion cells. The former shows a distinct maximum over time for oxidative peak currents, with CV peaks decaying after ~600 s for this par-

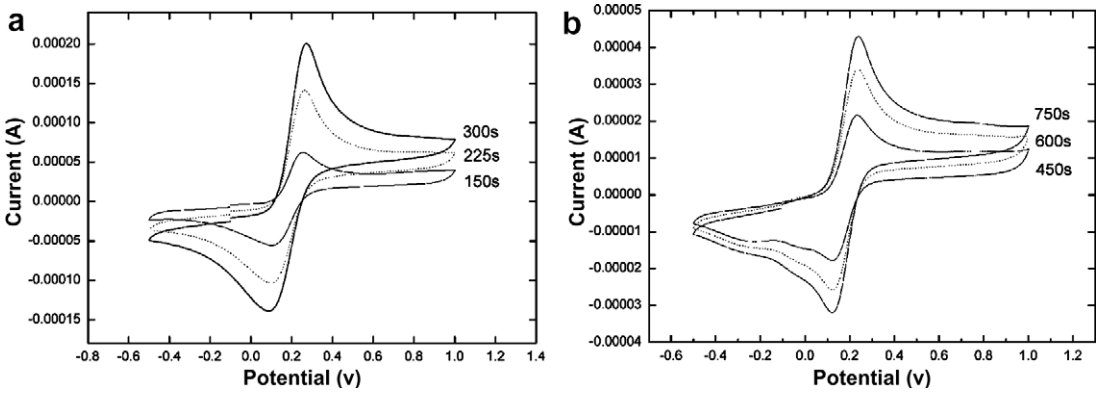

Fig. 5. The short-time increase in the amplitude of CVs obtained at the times indicated using (a) the Rank cell and (b) the diffusion cell. The peak currents are less in the diffusion cell than those measured in the Rank cell.

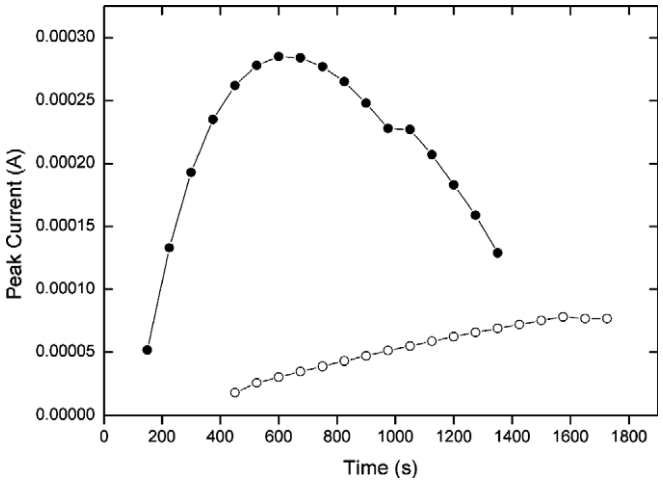

Fig. 6. A comparison of the time dependent oxidation peak current in the Rank cell (●) and in the diffusion cell (○).

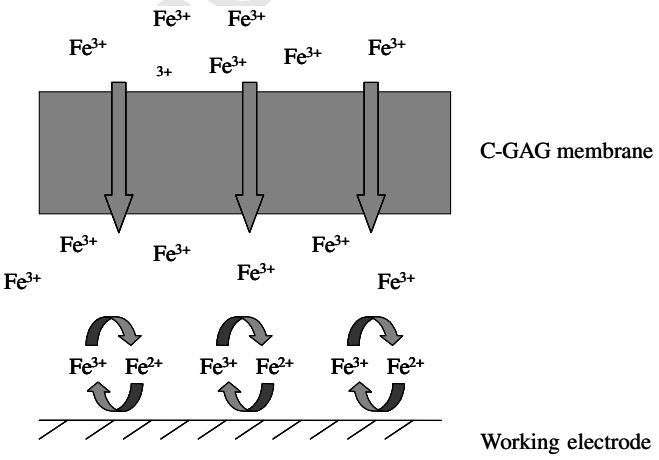

Fig. 7. The concentration of redox couple in the initial 200 nm range of the working electrode is determined by the rate at which it diffuses through the C-GAG membrane.

ticular sample. Corresponding measurements made using the diffusion cell show an almost linear increase in intensity, although, as previously stated, the oxidative peak current in the diffusion cell is lower than that measured in the Rank cell.

According to the Randles–Sevčik function, Eq. (2), any changes in the peak current, i_p, for a given experimental system are proportional to the concentration of the redox couple, the area of the working electrode and the diffusion coefficient of oxidizable molecules in the immediate vicinity of the working electrode. We therefore would expect a progressive increase in i_p with time for both experimental arrangements due to diffusion of the ferrocyanide though the C-GAG samples. Whilst this is the case for the diffusion cell data, it appears not to be so for the Rank cell. This suggests that some change in the local environment of the working electrode occurs; one likely explanation is that the C-GAG may collapse over time, forming a denser barrier layer that resists solute transport.

Fig. 7 shows a schematic representation of the diffusion of the redox couple through the C-GAG membrane and activity at the working electrode. The concentration of redox couple in the PBS buffer will increase with time due to diffusion across the C-GAG membrane. This will be detected by a change in the concentration of the redox couple very close to the electrode surface, potentially in a thin electrolyte film between the electrode and the C-GAG layer. The oxidation/reduction processes that give rise to the CVs occur within this narrow distance, and therefore the diffusion coefficient of the redox couple will be independent of the presence of a sample, i.e. changes in i_p are simply proportional to changes in the concentration of redox couple in this interfacial zone. Assuming this is the case, the experimental arrangement can be used as a means of gauging the flux of ferrocyanide through the gel membrane, with the external bulk solution concentration essentially unchanged.

By contrast, it is important to note that the concentration of the electroactive species in chamber A of the diffusion cell changes significantly with time, since a large volume of buffer is contained in chamber B. The need for concentration correction can be avoided provided only short-time data are considered (<400 s). This dilution issue is not a concern for the Rank cell since the volume between

the sample and the working electrode is much less than the volume of solution above.

3.4. Control matrix

Fig. 8 shows cyclic voltammograms with the Nuclepore® membrane in place using the Rank cell. From this figure it is clear that the presence of a membrane inhibits the response of the electrode to the redox couple despite the large size of the pores in comparison to the molecular probe. There is also an increase in response as the pore size increases. If degradation of the C-GAG matrix retains the internal structure whilst reducing the material content, we would expect to see an increased signal response from the electrode as the effective pore size increased. If the internal structure fails and collapses, this is likely to decrease the effective pore size and reduce the signal response.

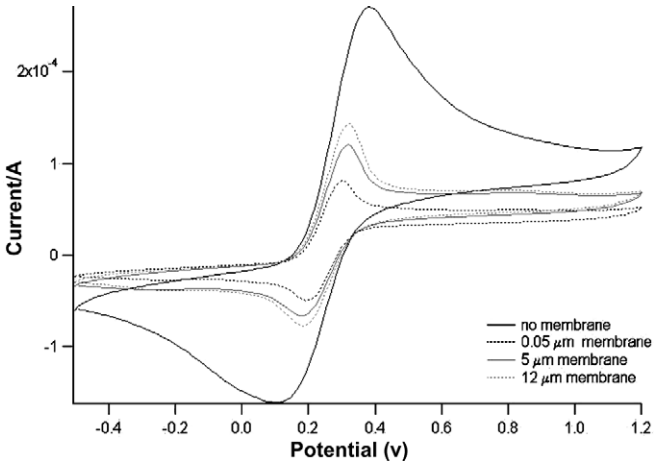

Fig. 8. The effect of membrane pore size on permeability measured using cyclic voltammetry and a standard redox couple ($K_4(FeCN)_6$).

3.5. The C-GAG matrix and degradation

Fig. 9a shows a micrograph of the original C-GAG matrix. This image shows a complex porous structure that appears to have gossamer-like sheets of C-GAG copolymer. The pores visible in the micrographs are relatively large – on a scale of 50–100 μm – but the structure suggests that solute passage from one side of the membrane to the other may be tortuous. The electron micrograph shown in Fig. 9b from an irradiated sample shows a comparable structure, i.e. any immediate changes that may result from irradiation do not alter the appearance of the microstructure, although it does show signs of filament formation. In contrast, the micrographs of an irradiated C-GAG matrix that has been incubated with collagenase (Figs. 9c and d) show a fibrous structure with little evidence of the original C-GAG sheets. This modified structure appears to be much more open than either the native or irradiated material.

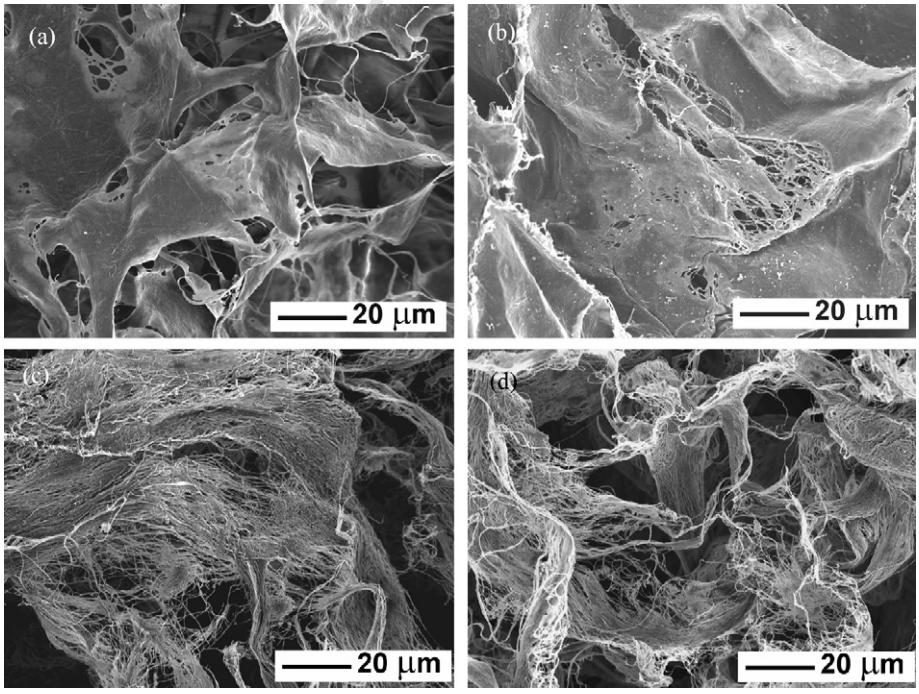

Fig. 9. Scanning electron micrographs of (a) non-degraded collagen/GAG matrix revealing a highly porous structure composed of sheet-like walls, (b) irradiated C-GAG sample (dose = 50 kGy) incubated at 37 °C, pH 7.4, very similar to the non-irradiated material but showing signs of filament formation; (c, d) irradiated C-GAG sample (dose = 50 kGy) incubated at 37 °C, pH 7.4, in the presence of collagenase (10 μg ml^{-1} in PBS), an open structure composed of sheaths of fibres.

Please cite this article in press as: Willows A et al., Assessment of tissue scaffold degradation using ..., Acta Biomater (2007), doi:10.1016/j.actbio.2007.10.009

3.6. Effect of degradation on the CVs of degraded C-GAG

The following sections show the effect that temperature conditioning, exposure to enzymes, storage at different pHs and protein adsorption have on CVs measured using the Rank cell (Fig. 2). This apparatus was chosen in preference to the diffusion cell because of the larger measured currents.

3.6.1. Effect of temperature

Fig. 10 shows a comparison of the peak oxidation current, i_p, measured in the Rank cell for C-GAG samples that were exposed to different levels of radiation and stored for a period of 48 h at 37 and 44 °C, respectively, with that of a control for comparison. The results from the irradiated samples show quite different behaviour to that of the control materials (Fig. 12). There is a slight increase in i_p over a period of about 30 min which is then essentially maintained independent of time. The magnitude of this current does not appear to correlate with the radiation exposure level or the incubation temperature (Fig. 11). Although no change is evident due to irradiation in the SEM images (Fig. 9b), the altered permeability is possibly the result of additional crosslinks forming and leads to a fall in ferrocyanide transport. The magnitude of i_p for the degraded material is about 1/3 of the maximum for the non-irradiated control. Irrespective of the variability in results, the radiation/thermal treatment of the C-GAG matrix appears to lead to stabilized structures without the transient effects seen for the original material. The possibility remains that

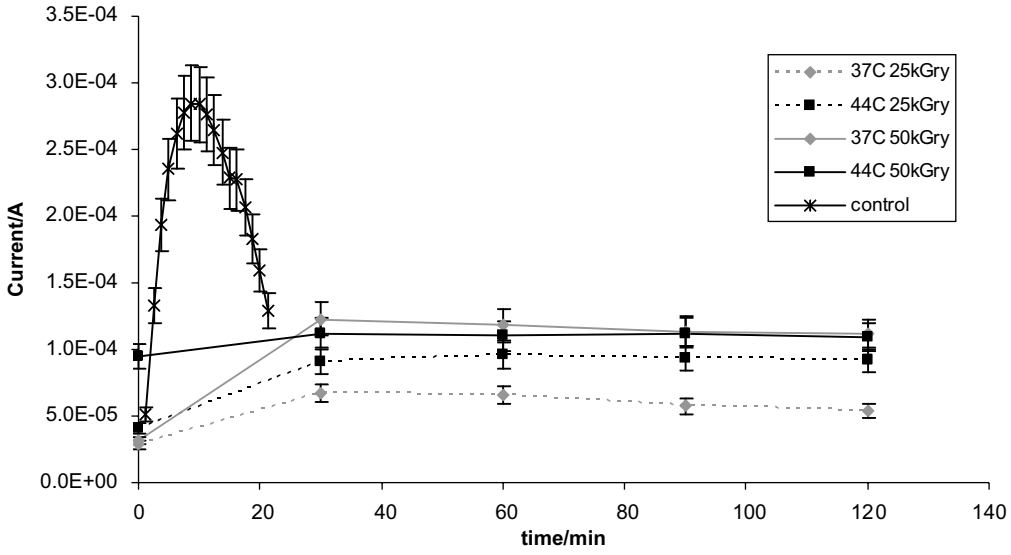

Fig. 10. A comparison of the time dependence of the oxidation peak current, i_p, for a non-irradiated C-GAG control stored at 4 °C with samples exposed to different levels of radiation, i.e. 25 or 50 kGy, and incubated at different temperatures for a period of 48 h.

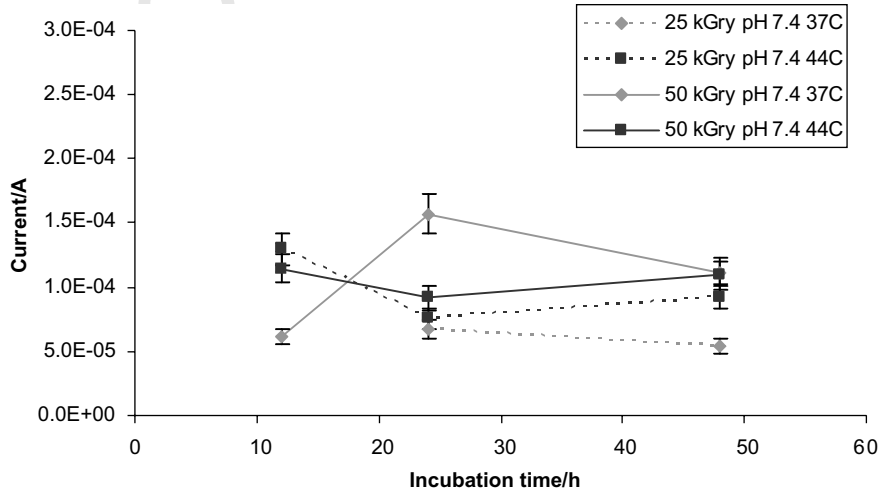

Fig. 11. The oxidation peak current, i_p, as a function of incubation time at different temperatures for samples that have been exposed to different levels of radiation.

Please cite this article in press as: Willows A et al., Assessment of tissue scaffold degradation using ..., Acta Biomater (2007), doi:10.1016/j.actbio.2007.10.009

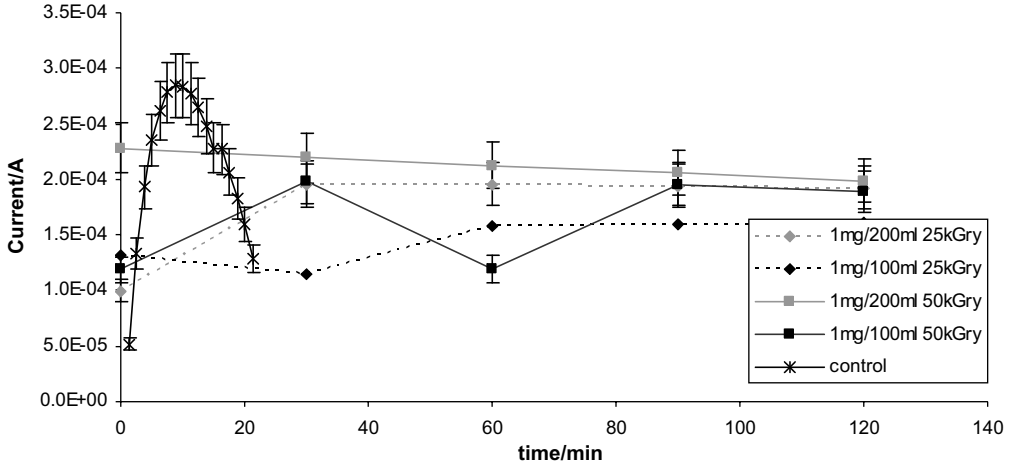

Fig. 12. Effect of collagenase concentration vs. time for irradiated samples after conditioning at 48 h.

changing the external solution changed the degree of gel swelling for the native material, though this should also have been evident for the two-compartment system (Fig. 6). Alternatively, the thin internal liquid film between the membrane and working electrode could have been diluted by buffer trapped in the C-GAG, or was compressed to a different degree over time due to the method used to clamp the sample in the cell.

3.6.2. Effect of collagenase

Fig. 12 shows the change in the magnitude of the oxidation peak as a function of time for irradiated samples that had been incubated with different amounts of collagenase for a period of 48 h. These results show that the measured current is essentially independent of time, which indicates that, as above, the samples remain stable in ferrocyanide solution. No clear i_p differences in radiation or collagenase effects are evident, but overall collagenase-treated samples tended to give higher i_p values, with greater permeability to ferrocyanide (Fig. 13).

3.6.3. Effect of pH

Fig. 14 suggests that the permeability of the C-GAG membrane is sensitive to the pH of the storage solution. Irradiated samples stored at pH 7 showed behaviour comparable to samples stored at elevated temperatures or exposed to collagenase. However, samples stored at pH 5 had very low oxidative peak currents. These materials appeared to structurally collapse onto the working electrode, presumably creating a lower porosity and denser structure.

4. Discussion

Two experimental approaches have been investigated to determine the permeability of hydrogel-like membranes to small molecular probes: a two-compartment diffusion cell and a single-compartment Rank cell. At first sight, the two-compartment cell in which the sample is located well away from the electrodes has a significant advantage over the Rank cell as it avoids any complica-

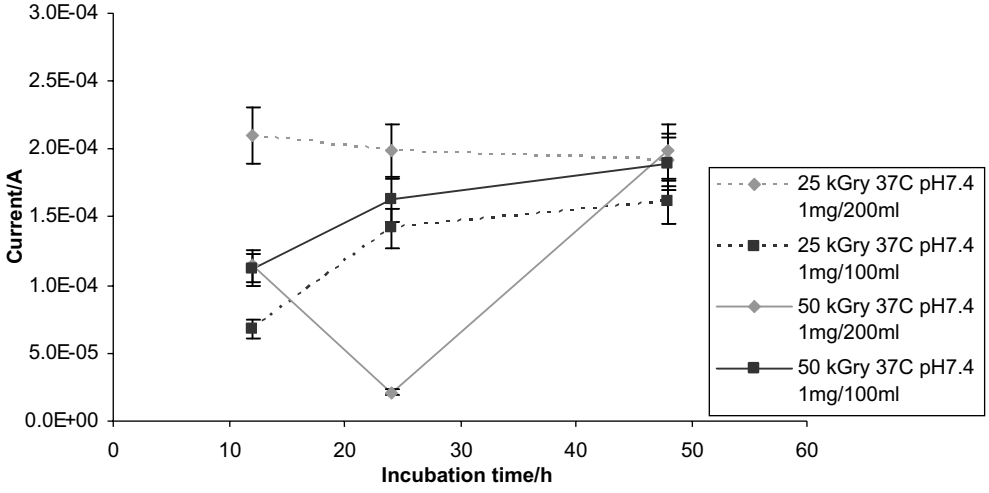

Fig. 13. The effect of different conditioning times (12, 24 and 48 h) on the CVs of irradiated samples incubated with different concentrations of collagenase.

Please cite this article in press as: Willows A et al., Assessment of tissue scaffold degradation using ..., Acta Biomater (2007), doi:10.1016/j.actbio.2007.10.009

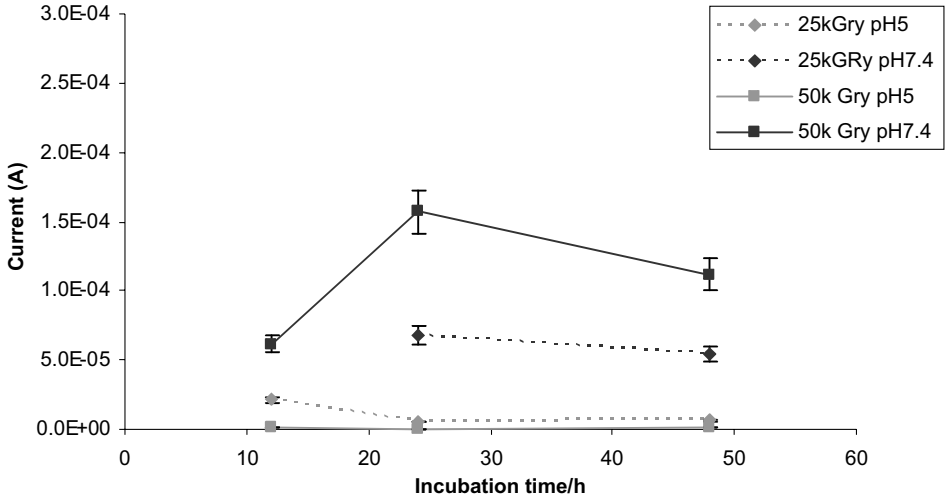

Fig. 14. The effect of pH on the permeability of irradiated C-GAG samples to ferrocyanide.

tions due to sample collapse on to the working electrode. However, due to dilution effects measured currents in the diffusion cell are much lower than those measured in the single-compartment Rank cell. A further practical consideration is that the two-compartment diffusion cell has to be filled with fluid at the same rate in each chamber to avoid flow due to pressure differences. Ferrocyanide transfer across the membrane (Fig. 1) also reduces the magnitude of the diffusion gradient between the two chambers.

In the single-compartment Rank cell, the sample is sited directly over the working electrode and, while this minimizes the volume of buffer sampled, the volume of solution containing electroactive species above the sample is also low (1 cm^3) to minimize the pressure acting on the sample. This relatively small volume of solution could easily become diluted with buffer volume already contained within the sample and this, together with gel swelling or compression, could influence the reproducibility and accuracy of quantitative measurements based on CVs. Furthermore, the system may be susceptible to greater electrode surface fouling, i.e. the functional area of the working electrode may be reduced through intimate contact with the sample or through protein adsorption.

Exposure to radiation and storage under different environments that are designed to accelerate the rate of degradation of the C-GAG matrix can in principle produce a significant change in the structure of a material. Exposure of the native material to different doses of radiation appears to stabilize the initial structure, though no dose- or temperature-correlated effects were seen. Exposure of the material to collagenase had significant effects on the structure, converting the sheet-like domains into fibrous meshes with a tendency to increased permeability. This contrasts with the marked evidence of structural collapse at pH 5. In terms of the measured CVs, irradiated samples, thermally conditioned irradiated samples and irradiated samples treated with collagenase all significantly increase the permeability of C-GAG scaffolds to ferrocyanide. This increased permeability is independent of the measurement time and incubation time, suggesting that the treated hydrogels are much more permeable than the native material.

Storing irradiated samples in an acidic environment (pH 5) or in a solution containing fibrinogen has a significant effect on measured CVs, reducing the oxidation peak current to very low levels. This behaviour might be explained by collapse of the sample onto the working electrode surface (pH 5 storage).

5. Conclusions

An electrochemical redox probe allowed investigation of the change in permeability of a collagen–glycosaminoglycan dermal equivalent matrix due to various degradation conditions. Collagenase-treated C-GAG samples show a change in structure and increased permeability. Storing irradiated samples in an acidic environment (pH 5) or with fibrinogen appears to cause a degree of collapse within the structure and decreases permeability. These factors should be taken into account during sterilization and storage of the dermal equivalent matrix.

Acknowledgements

We thank Jaroslaw Wasikiewicz, of Queen Mary, University of London, for experimental assistance. This work was funded by the United Kingdom Department of Trade and Industry as part of the Measurements for Processability and Performance of Materials (MPP) programme.

References

[1] Wallace DG, Rosenblatt JL. Collagen gel systems for sustained delivery and tissue engineering. Drug Deliv 2003;55:1631–49.

[2] Vernon RB, Gooden MD, Lara SL, Wight TN. Native fibrillar collagen membranes of micron-scale and submicron thickness for cell support and perfusion. Biomaterials 2005;26:1109–17.
[3] Lin ASP, Barrows TH, Cartmell SH, Guldberg RE. Microarchitectural and mechanical characterization of oriented porous polymer scaffolds. Biomaterials 2003;24:481–9.
[4] Ho ST, Hutmacher DW. A comparison of micro CT with other techniques used in the characterization of scaffolds. Biomaterials 2006;27:1362–76.
[5] Wang HJ, Pieper J, Peters F, van Blitterswijk CA, Lamme EN. Synthetic scaffold morphology controls human dermal connective tissue formation. J Biomed Mater Res Part A 2005;74A:523–32.
[6] Kanaya T, Takeshita H, Nishikoji Y, Ohkura M, Nishida K, Kaji K. Micro- and mesoscopic structure of poly(vinyl alcohol) gels determined by neutron and light scattering. Supramol Sci 1998;5:215–21.
[7] Svergun DI, Koch MHJ. Small-angle scattering studies of biological macromolecules in solution. Rep Prog Phys 2003;66:1735–82.
[8] Ismail F, Willows A, Khurana M, Tomlins PE, James S, Vadgama P, et al. A test method to monitor in vitro storage and degradation effects on a skin substitute. Med Eng Phys; in press.
[9] Yannas IV, Lee E, Orgill DP, Skrabut EM, Murphy GF. Synthesis and characterization of a model extracellular-matrix that induces partial regeneration of adult mammalian skin. Proc Nat Acad Sci USA 1989;86:933–7.
[10] Jarman-Smith ML, Bodamyali T, Stevens C, Howell JA, Horrocks M, Chaudhuri J. Porcine collagen crosslinking, degradation and its capability for fibroblast adhesion and proliferation. J Mater Sci – Mater Med 2004;15(8):925–32.
[11] Harley BA, Spilker MH, Wu JW, Asano K, Hsu HP, Spector M, et al. Optimal degradation rate for collagen chambers used for regeneration of peripheral nerves over long gaps. Cells Tissues Organs 2004;176:153–65.
[12] Gordon TD, Schloesser L, Humphries DE, Spector M. Effects of the degradation rate of collagen matrices on articular chondrocyte proliferation and biosynthesis in vitro. Tissue Eng 2004;10:1287–95.
[13] Van Amerongen MJ, Harmsen MC, Petersen AH, Kors G, van Luyn MJA. The enzymatic degradation of scaffolds and their replacement by vascularised extracellular matrix in the murine myocardium. Biomaterials 2006;27:2247–57.
[14] Miles CA, Sionkowska A, Hulin SL, Sims TJ, Avery NC, Bailey AJ. Identification of an intermediate state in the helix-coil degradation of collagen by ultraviolet light. J Biol Chem 2000;275:33014–20.
[15] Wang XN, Li XD, Yost MJ. Microtensile testing of collagen fibril for cardiovascular tissue engineering. J Biomed Mater Res Part A 2005;74A:263–8.
[16] Benson RS. Use of radiation in biomaterials science. Nucl Instrum Methods Phys Res B 2002;191:752–7.
[17] Pratt CM, Barton S, McGonigle E, Kishi M, Foot PJS. The effect of ionising radiation on poly(methyl methacrylate) used in intraocular lenses. Polym Degrad Stabil 2006;91:2315–7.
[18] Pek YS, Spector M, Yannas IV, Gibson LJ. Degradation of a collagen–chondroitin-6-sulfate matrix by collagenase and by chondroitinase. Biomaterials 2004;25:473.
[19] Holy CE, Dang SM, Davies JE, Shoichet MS. In vitro degradation of a novel poly(lactide-co-glycolide) 75/25 foam. Biomaterials 1999;20:1177.
[20] Compton CC, Butler CE, Yannas IV, Warland G, Orgill DP. Organized skin structure is regenerated in vivo from collagen–GAG matrices seeded with autologous keratinocytes. J Invest Dermatol 1998;110:908–16.
[21] British Pharmacopoeia Commission. British Pharmacopeia 2008. London: The Stationery Office; 2007.
[22] Hibbert B, James AM. Dictionary of electrochemistry. London: Macmillan Press; 1984.
[23] Bard AJ, Faulkner LR. Electrochemical methods: fundamentals and applications. New York: Wiley & Sons; 2001.
[24] Sawyer DT, Sobkowiak A, Roberts JL. Electrochemistry for chemists. New York: Wiley & Sons; 1995.